Change Detection for Monitoring Forest Defoliation

Douglas M. Muchoney and Barry N. Haack

Abstract

Monitoring of environmental conditions such as forest defoliation by insects over large areas is facilitated by automated approaches to change detection using remotely sensed data. This study evaluated four change detection techniques using multispectral, multitemporal SPOT data for identifying changes in hardwood forest defoliation caused by gypsy moth, Lymantria dispar *L.*

The change detection techniques considered were principal components analysis, image differencing, spectral-temporal (layered temporal) change classification, and post-classification change differencing. The study area comprised approximately 148 square kilometres in Warren and Shenandoah Counties, Virginia. Reference information of defoliation were aerial sketch maps developed by the U.S. Forest Service.

Results indicate that defoliation may be best determined by image differencing and principal components analysis. A pair-wise test of significance determined that the four techniques resulted in significantly different accuracies at a 95 percent probability level. Principal components and image differencing analyses are generally more complex than post-classification because data no longer represent actual sensor data values, and classification involves identifying change, rather than cover, classes. These techniques are simpler than post-classification approaches, which require independent classification prior to change detection.

Introduction

A significant insect defoliation problem in the United States is caused by the gypsy moth, *Lymantria dispar* L. Defoliation assessment commonly involves aerial sketch mapping, photographic interpretation, and/or ground surveys. These techniques can be subjective and labor intensive. Automated change detection using satellite data could allow for timely and consistent estimates of defoliation trends over large areas, and ease of data capture into a Geographic Information System (GIS).

Forest assessments for monitoring gypsy moth defoliation require data acquisition at least once during the early summer when the insects are most active. Subsequent data acquisitions are also necessary to characterize regrowth and re-infestation during the growing season and to monitor suppression activities (Ciesla, 1981). Because defoliation can occur over thousands of hectares, there is also the need to have a synoptic view of defoliation (Talerico *et al.*, 1978).

Satellite-based digital remote sensing has been used for forest cover type mapping (Nash *et al.*, 1980; Bryant *et al.*, 1980; Buchheim *et al.*, 1984), forest clearing (Sader, 1987), silvicultural assessments (Tom and Miller, 1980), disturbance assessment and monitoring (Aldrich, 1975), and forest defoliation and damage assessment studies (Nelson, 1983; Vogelmann and Rock, 1988; Vogelmann and Rock, 1989). The defoliation assessment studies have included damage from insects such as Mountain Pine Beetle, *Dendroctonus ponderosae* (Sirois and Ahern, 1989); Hemlock Looper, *Lambdina fiscellaria fiscellaria* (Franklin, 1989); and Spruce Budworm, *Choristoneura fumiferana* Clemens (Buchheim *et al.*, 1984); as well as gypsy moth (Nelson, 1983; Ciesla *et al.*, 1989).

Landsat Multispectral Scanner (MSS) and Thematic Mapper (TM) data have been used successfully to map forest defoliation for a single date. Rohde and Moore (1974) delineated gypsy moth defoliation using false color composites of Landsat MSS data, and enhanced defoliation estimates with multitemporal MSS band 7 composites. Johnson (1980) evaluated an iterative procedure using an unsupervised clustering algorithm to develop training statistics for forest and non-forest categories using Landsat MSS data including three levels of canopy defoliation. Reported accuracies were 82.0 percent plus/minus 2.4 percent.

Williams *et al.* (1985) used ratio vegetation indices of Landsat MSS bands 5 and 7 to discriminate heavy forest defoliation from a category of moderate defoliation and healthy forest with accuracies of 75 to 80 percent. Williams and Nelson (1986) developed techniques to delineate and assess forest damage due to defoliating insects with a reported 90 percent classification accuracy for delineating insect-damaged and healthy forest. Vogelmann and Rock (1988) evaluated Landsat TM data for its ability to detect and measure damage to spruce-fir stands. That study indicated that TM Band 5/4 and 7/4 ratios correlated well with ground observations of forest damage defined as percent foliar loss.

Applications of forest monitoring using SPOT (Satellite Probatoire pour l'Observation de la Terre) include the evaluation of simulated SPOT data for their ability to map forest cover type and detect defoliation caused by the spruce budworm (Buchheim *et al.*, 1984). That study found that, although defoliation was discernible using digital processing, contextual information was needed to discriminate forest cover type. SPOT-XS (multispectral) color composites have also been used to delineate areas of gypsy moth defoliation

Department of Geography, George Mason University, Fairfax, VA 22030.

D. M. Muchoney's present address is The Nature Conservancy, 1815 North Lynn Street, Arlington, VA 22209.

Photogrammetric Engineering & Remote Sensing, Vol. 60, No. 10, October 1994, pp. 1243–1251.

0099-1112/94/6010-1243$3.00/0

in eastern hardwood forests (Ciesla *et al.*, 1989). The authors compared defoliation estimates obtained from panoramic color infrared (CIR) aerial photography and reported an overall agreement between the two methods as 86 percent, although there were differences between the two techniques in their ability to classify defoliation intensity.

Change detection using multitemporal data had previously been employed primarily for the evaluation of land-cover changes associated with urbanization (Christenson and Lachowski, 1976; Wickware and Howarth, 1981; Estes *et al.*, 1982), desertification (Coiner, 1980; Robinove *et al.*, 1981), and coastal zone monitoring (Weismiller *et al.*, 1977; Hong and Iisaka, 1982). Specific applications of change detection to monitoring defoliation include Nelson (1983), who evaluated image differencing, ratioing, and vegetative index differencing of Landsat MSS data for detecting defoliation due to gypsy moth. That study concluded that the vegetative index differencing and an MSS Band 5 ratio gave the best indication of forest canopy change, with accuracies of about 78 percent. Vogelmann and Rock (1989) used multitemporal Landsat TM band 4 image differencing (subtraction) with single-date band 3 and 5 data to distinguish between high and low levels of defoliation of hardwood forests caused by the Pear Thrips, *Taeniothrips inconsequens* Uzel.

The objective of this study was to evaluate four change detection techniques using multitemporal, multispectral satellite data to identify changes in hardwood forest defoliation caused by gypsy moth. The four methods were (1) principal components analysis (PCA), (2) image differencing (ID), (3) spectral-temporal change classification (STCC), and (4) post-classification change detection differencing (PCCDD).

SPOT XS multispectral data for two years, 1987 and 1988, were obtained for portions of Warren and Shenandoah Counties, Virginia. Criteria for evaluating the change detection techniques were classification accuracy, signature development complexity, data reduction, and processing and analysis intensity.

Study Area

The study area comprised a portion of the Strasburg, Virginia 1987 U.S. Geological Survey (USGS) 7.5-minute quadrangle map including approximately 148 square kilometres or 57 square miles (Figure 1). The study area is located within both the Blue Ridge Physiographic Province, and the Appalachian Valley and Ridge Physiographic Province. The Valley and Ridge Province comprising the western portion of the study area includes Massanutten Mountain and the adjacent foot slopes, narrow ridges, flood plains, and uplands. The rock strata in this region are predominantly folded sandstone, siltstone, and limestone. In the eastern portion of the study area, the steep to moderately steep foothills are underlain by greenstone and granitic rock (Holmes *et al.*, 1984).

The forest cover of the region is predominantly hardwood and mixed oak-pine in the upland forested regions. The dominant tree species present are white oak (*Quercus alba* L.), northern red oak (*Quercus rubra* L.), chestnut oak (*Quercus prinus* L.), shagbark hickory (*Carya ovata* (Mill.) K. Koch), and American beech (*Fagus grandifolia* Ehrh.) (Smith and Linnartz, 1980). Lower elevations support agricultural crops and pasturage.

The upland hardwood forests of the region, including the study area, have been recently disturbed by the invasion of gypsy moth. Gypsy moth eggs are laid during the summer season and hatch the following spring. These first-stage larvae feed primarily on oaks (*Quercus* spp.) and other hardwoods, particularly walnut (*Juglans* spp.), basswood (*Tilia* spp.), and birch (*Betula* spp.). The optimum time to evaluate the effects of gypsy moth defoliation is 1 to 21 June, when gypsy moth infestation is at its peak (Knight and Heikkenen, 1980; Ciesla *et al.*, 1989).

Methodology

SPOT Haute Resolution Visible (HRV) XS data were acquired on 15 June 1987 and SPOT HRV-XS and panchromatic data (PAN) were acquired on 4 July 1988 (Path-Row KJ 619, 272). Although the 1988 data were acquired two weeks after what is considered to be the peak of infestation, it is not late enough to allow for vegetation to recover and defoliation would still be quite evident.

The multispectral data from June 1987 and 1988 were geocoded and resampled from 20-metre to 10-metre spatial resolution using an intensity, hue, and saturation (IHS) transformation based on the SPOT 10-metre panchromatic data. The geocoding process used a single set of control points to create a sensor-orbit-Earth ellipsoid model to transform individual pixels to the Universal Transverse Mercator (UTM) reference system. The geocoding also employed a 1:25,000-scale terrain model (50-metre contour) to remove terrain relief distortions. A nearest-neighbor spatial interpolation was used to retain radiometric integrity, and the root-mean-square of the rectification model was approximately one pixel (ten metres).

Precision geocoding of the multitemporal data obviated additional resampling for image-to-image co-registration. Precise co-registration of the data sets is critical to minimize misregistration that might provide false indications of image-to- image change. No corrections for atmospheric effects were performed because the imprecision of a scattering model might influence change detection results. This also enabled characterization of each change detection technique's ability to isolate inter-image variance due to atmospheric effects. At the resampled spatial resolution of 10 metres, 1088 rows by 1391 scan lines, or 1,513,408 pixels, were included.

Defoliation maps of the study area had been developed by the U.S. Forest Service from aerial sketch mapping performed in June of 1987 and 1988. These maps corresponding to the U.S. Geological Survey 7.5-minute, 1:24,000 scale topographic map were obtained and digitized into a raster GIS (Figure 1). The 1988 defoliation maps were classified by the Forest Service as non- defoliated (greater than or equal to 30 percent defoliation), moderate defoliation (31 to 60 percent defoliation), and heavy defoliation (61 to 100 percent defoliation. Because the 1987 data maps included only defoliated/non-defoliated classes, the 1988 data were recoded also as defoliated/non-defoliated, with moderate defoliation included as defoliation.

The minimum mapping unit of the defoliation polygons was approximately 4 hectares (10 acres). These sketch maps were the reference information for the accuracy evaluation of the change detection strategies. No quantitative assessment of the accuracy of the sketch maps was performed. These techniques are generally assumed to be reliable indicators of defoliation due to gypsy moth, although sketch-mapping can be inaccurate (Aldrich *et al.*, 1958). Thus, accuracy assessment should be considered as relative, rather than absolute, when evaluating the four change detection methods.

Principal Components Analysis

PCA, or the Karhunen-Loeve (K-L) transformation (Duvernoy and Leger, 1980), is a multivariate statistical technique where data axes are rotated into principal axes, or components, that

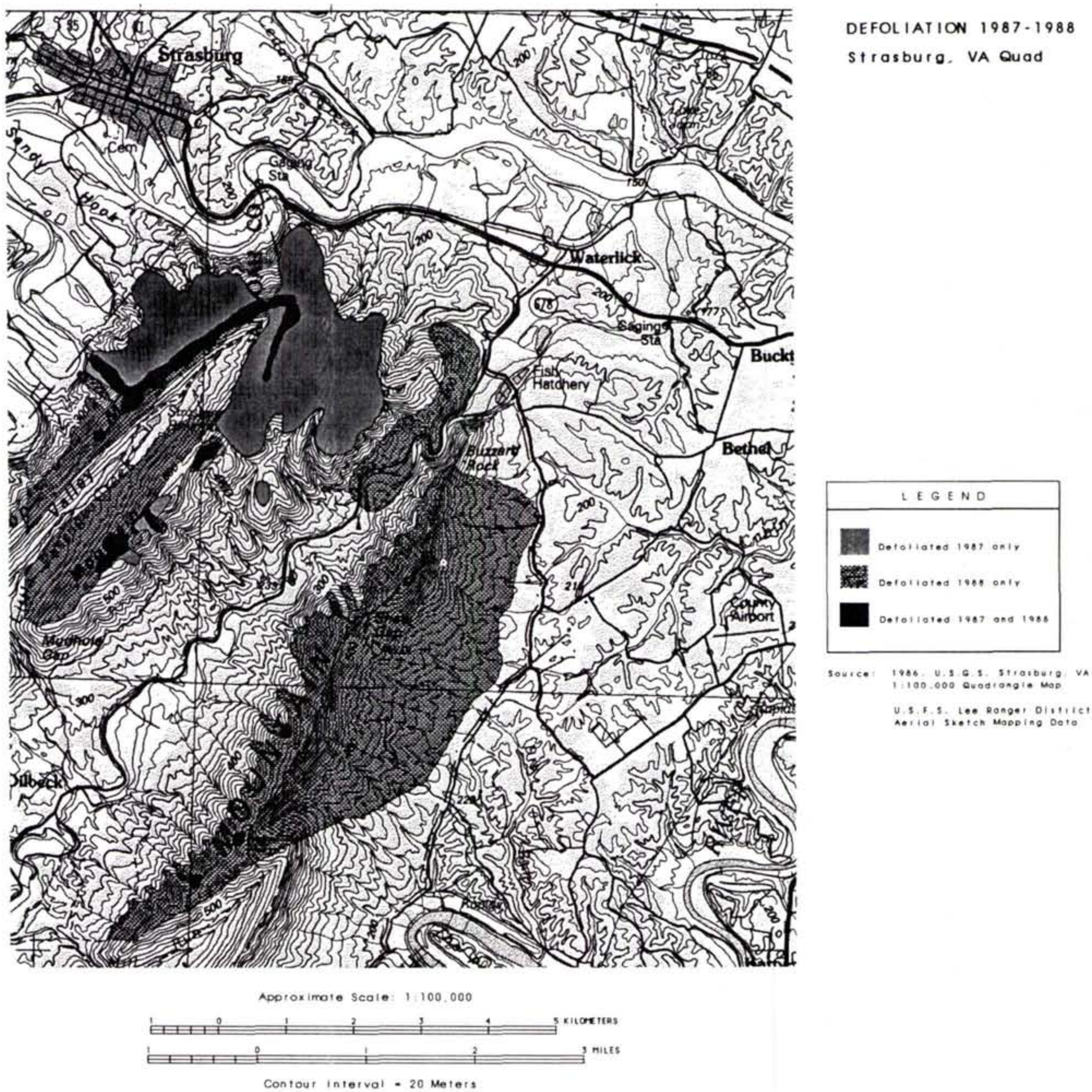

Figure 1. Study area.

maximize data variance (Figure 2). The original data are then transformed to the new principal axes, or components. In this manner, correlated data sets can be represented by a smaller number of axes, while maintaining most of the variation of the original data. For change detection purposes, PCA can be divided into two categories: (1) independent and (2) merged data transformation and analyses. Independent transformations are subsets of post-classification change detection that employ PCA independently on registered temporal data pairs as a prelude to post-classification comparisons (Estes *et al.*, 1982). Merged data transformations are those that rely upon PCA of combined multitemporal data sets to isolate inter-image change. The premise for this analysis is that multitemporal data sets are highly correlated and that PCA can be used to highlight differences attributable to change (Byrne *et al.*, 1980).

PCA for this study was based on the entire merged data set. The eigenvalue matrix (Table 1) indicates that eigenimage 1 accounts for the majority of the inter-image variance - 61.3 percent. Eigenimages 2, 3, and 4 account for 22.9, 9.3, and 5.6 percent of the inter-image variance, respectively. The remaining two components, 5 and 6, account for less than 1

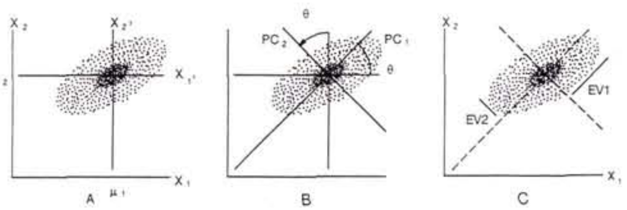

Figure 2. Principal component transformation. (A) Bivariate scatterplot with mean and new coordinate system. (B) Construction and rotation of the principal components with theta equal to the angle of rotation and variance optimized by angle. (C) Component eigenvectors (EV), where the lengths of the eigenvectors are the eigenvalues (from Jensen, 1986; Jensen and Waltz, 1979).

Table 1. Merged Principal Components

Covariance Matrix

Band1/87	Band2/87	Band3/87	Band1/88	Band2/88	Band3/88
1203.02	1328.53	−568.68	1268.97	1292.90	−476.16
	1572.17	−844.35	1468.83	1521.16	−599.75
		3149.52	−1021.22	−1130.17	1999.03
			2668.23	2700.79	−1168.85
				2913.91	−1381.43
					3278.24

Correlation Matrix

Band1/87	Band2/87	Band3/87	Band1/88	Band2/88	Band3/88
1.000	0.966	−0.292	0.708	0.691	−0.240
	1.000	−0.379	0.717	0.711	−0.264
		1.000	−0.352	−0.373	0.622
			1.000	0.969	−0.395
				1.000	−0.447
					1.000

Eigenvalues

Eigenimage	Eigenvalues	Var. %	Total %	Angle
1	9065.319	61.314	61.314	72.106
2	3385.380	22.897	84.211	19.434
3	1380.770	9.339	93.550	93.577
4	831.676	5.625	99.175	96.288
5	84.992	0.575	99.750	89.382
6	36.934	0.250	100.000	89.025

Eigenvectors

0.271	0.250	−0.270	−0.	−0.161	0.719
0.324	0.249	−0.369	−0.494	0.163	−0.653
−0.393	0.572	0.624	−0.354	0.005	−0.061
0.483	0.333	0.177	0.331	−0.700	−0.158
0.514	0.306	0.236	0.322	0.675	0.163
−0.412	0.587	−0.561	0.411	0.039	0.035

percent of this variance. Analysis of the eigenvector matrix indicates the relative contribution to the overall eigenimage variance by each of the image bands. This "factor loading analysis" provides insight into how each image band loads or contributes to the principal components transformation when considered with visual inspection of eigenimages.

Eigenimage 1 is attributable to changes in overall scene brightness, while eigenimage 2 represents changes in overall scene greenness (Figure 3). Eigenimage 3 is due to changes caused by forest defoliation, and other changes in vegetation cover which would impact infrared (IR) reflectance, such as cropping followed by fallow-field conditions. Eigenimage 4 is attributable to differences in the two images caused by clouds and cloud shadows being present in the first year only. The remaining two eigenimages, which account for only 0.83 percent of the inter-image variability, represent inter-image differences due to atmospheric and sensor variations. The sensor variations are evident in sensor band striping in these two eigenimages.

Two PCA approaches were developed. In the first, merged PCA (MPCA), all six principal components, or eigenimages, were used in performing an unsupervised statistical signature extraction based on minimum spectral distances and scaled cluster weight criteria and application of a Bayesian maximum-likelihood decision rule. For this and subsequent processing, 25 unsupervised signatures were generated. Although the six eigenimages contain all of the variance of the original six bands, this allowed the evaluation of the effects of the principal component transformation on classification accuracy. In the second approach, because eigenimage 3 (PC3) was found to represent year-to-year variance due to defoliation, it was also classified independently using density level slicing.

Image Differencing or Delta Change DetectionID is a technique whereby changes in brightness values between two or more data sets are determined by cell-by-cell subtraction of co-registered image data sets. The subtraction (differencing) produces an image data set where positive and negative values represent areas of change and values close to zero indicate areas that remain relatively unchanged. Threshold values are often defined and used to indicate whether significant or relevant change has occurred. This method requires that the difference image be normalized to the median of the quantization level. For these 8-bit data (0 to 255, or 256 levels) the median value (127) was added to the original value resulting from the subtraction.

The pixel-by-pixel subtraction of registered images resulting from image differencing can be used to create maps of increased and decreased values of the reflectance of surface features. In arid lands, for example, decreases in albedo may indicate site degradation or desertification (Robinove *et al.*, 1981). Image differencing can also be used to identify areas where further analysis might be required, thereby reducing the amount of ground referencing required for effective analysis by as much as 97 percent (Estes *et al.*, 1982). In this study, the data sets were subtracted band-by-band, normalized, and classified without using change thresholds (Plate 1).

Spectral-Temporal Change Classification

STCC, or layered temporal change detection, is based on single analysis of a merged multi-date data set using standard pattern recognition and classification techniques. Because the data sets would otherwise be similar, changes would be significantly different statistically (Weismiller *et al.*, 1977). Although this technique only requires a single classification, signature development can be very complex, especially when a large number of spectral bands are considered (Jensen, 1986).

STCC required merging the pre-processed data into a sin-

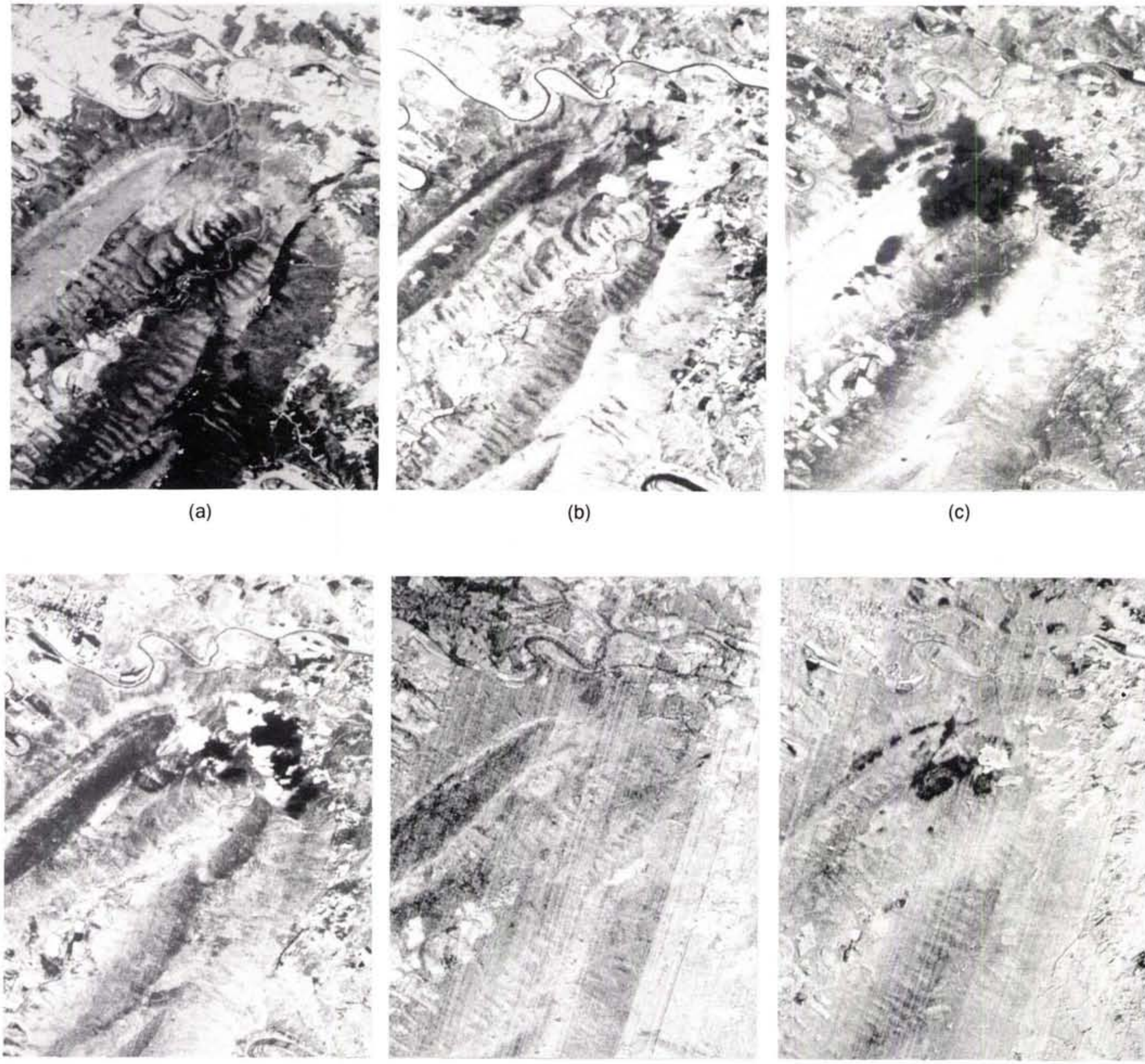

(a) (b) (c) (d) (e) (f)

Figure 3. Individual eigenimages. (a) PC1. (b) PC2. (c) PC3. (d) PC4. (e) PC5. (f) PC6.

gle six-band data set. Classification was performed by extracting unsupervised signatures and applying a maximum-likelihood decision rule.

Post-Classification Change Detection Differencing

PCCDD is a technique where multi-date digital data sets are independently classified and then compared on a pixel-by-pixel, or polygon-by-polygon, basis for each class (Wickware and Howarth, 1981). The classification maps are compared using class pairs as described by the analyst, and the result is an indicator of areas of change (Weismiller *et al.*, 1977; Estes *et al.*, 1982).

PCCDD was performed on the SPOT data sets using two approaches. In addition to the cluster-generated signatures, training classes were also defined interactively prior to the application of a maximum-likelihood decision rule.

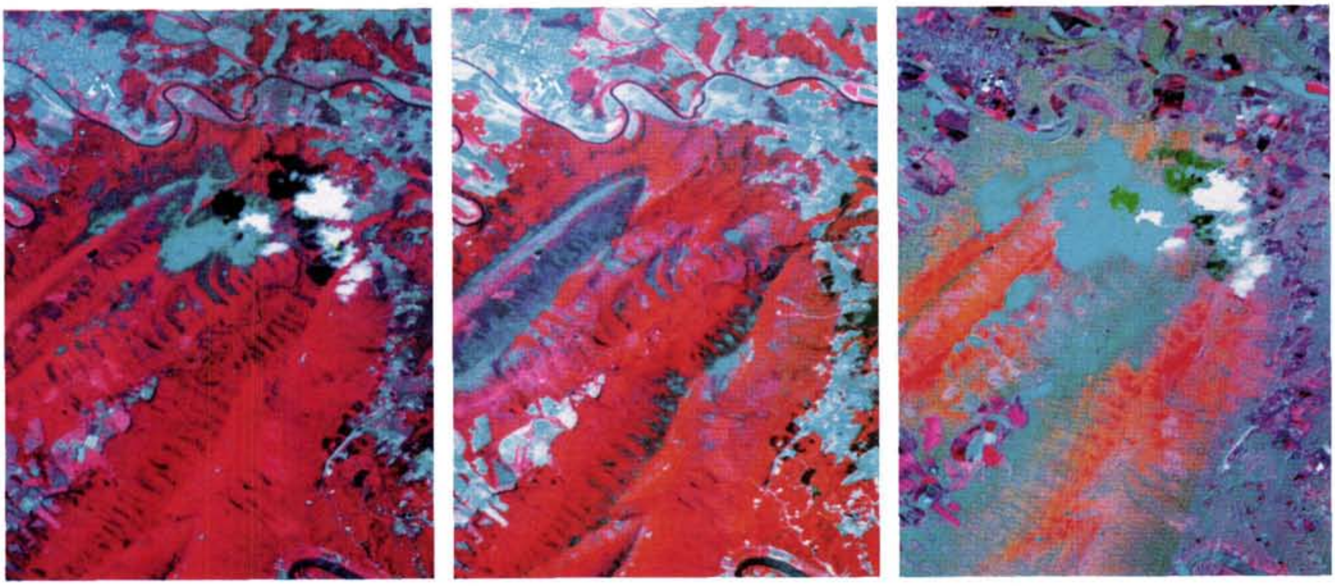

(a) (b) (c)

Plate 1. 1987, 1988 (RGB = 3, 2, 1; courtesy SPOT Image Corporation), and Image Differencing images (ID displayed as RGB = 1, 2, 3 for difference bands 1, 2, 3, respectively). (a) 1987 SPOT XS. (b) 1988 SPOT XS. (c) Image differencing.

Results and Discussion

One of the criteria for evaluating the change detection technique was classification accuracy. Accuracy assessment was performed using a GIS to reference the U.S. Forest Service aerial sketch mapping classification. The standard error matrices for the techniques are provided in Table 2. The overall accuracy as well as the normalized overall accuracy and Kappa Coefficient (KHAT) statistic, as described by Congalton *et al.* (1983) and Congalton (1991), are included as Table 3. The Kappa Coefficient was generated for each error matrix as an estimate of agreement where chance agreement is removed.

The Z-statistic was used as a pair-wise test of significance between the techniques at a 95 percent probability level (Congalton *et al.*, 1983). It indicated that the techniques differed significantly (Table 4.), that is, the absolute value of the test statistic was greater than 1.96. The accuracy ranking by technique varied somewhat according to whether the standard error matrix, normalized error matrix, or Kappa Coefficient was scrutinized, although image differencing and PC3 rank one and two, respectively, for all three. It is important to note that only PCCDD and STCC were capable of determining that defoliation occurred in both 1987 and 1988. Therefore, this category was not included in comparing the techniques.

Merged Principal Components Analysis

MPCA was intended to identify the single component image that reflected changes in defoliation, i.e., PC3. MPCA does, however, have the advantage of defining the source of other inter-image variance. Atmospheric effects and band striping were isolated as individual components. The accuracy of MPCA differed significantly from that of STCC, although the data were of the same dimensions and MPCA accounts for the same variance in the data as STCC. It is uncertain whether this difference is due to the effects of the principal components transformation or as a result of the unsupervised signature generation.

Improper generation of the transformation matrix is of primary concern when using MPCA. Creating subsets of the image data to guide transformation matrix generation so as to highlight features of interest can be employed with potentially good results (Duggin *et al.*, 1986), although there may be no prediction towards this end. Data correlation is determined by constructing either a covariance or a correlation matrix (Fung and LeDrew, 1987), and results can differ significantly according to which matrix is employed.

Principal Component 3

The PC3 analysis offered better locational accuracy results than did the MPCA. Defoliation in any one year was manifested at the tails of the PC3 smoothed frequency polygon (Figure 4). The optimum standard deviation-derived density level slice was determined by plotting relative classification accuracies (Figure 5). Although this procedure was based on using the reference data, sampling to calibrate the level slice could be performed. PCA has the best potential for becoming a truly automated change detection technique. The ability to discern defoliation was found to be based solely on distance from the data mean, and defining defoliation in any region was accomplished by setting the limits of the single-band density slice. It also obviates normalizing multitemporal data sets to remove inter-image variability due to sensor and atmospheric conditions and not due to change.

Image Differencing

ID offered the ability to define change thresholds and allows for flexible subsetting of data for classification improvement

TABLE 2. ERROR MATRICES

MPCA Error Matrix, Reference Data

Classified Data	Non-Def. 1987/88	Defol. 1987	Defol. 1988	Defol. 87/88	Totals
Non-Defoliated 1987 and 1988	325,688	37,454	108,378	7,322	478,842
Defoliated 1987 only	10,314	15,222	655	956	27,147
Defoliated 1988 only	66,319	4,749	74,320	4,381	149,769
Defoliated 1987 and 1988	0	0	0	0	0
Totals	402,321	27,147	149,769	12,659	655,758

PC3 Error Matrix, Reference Data

Classified Data	Non-Def. 1987/88	Defol. 1987	Defol. 1988	Defol. 87/88	Totals
Non-defoliated 1987 and 1988	305,114	16,358	95,244	4,508	421,224
Defoliated 1987 only	42,085	38,857	1,818	3,626	86,388
Defoliated 1988 only	55,122	2,210	86,291	4,525	148,148
Defoliated 1987 and 1988	0	0	0	0	0
Totals	402,321	57,425	183,352	12,659	655,758

Image Differencing Error Matrix, Reference Data

Classified Data	Non-Def. 1987/88	Defol. 1987	Defol. 1988	Defol. 87/88	Totals
Non-Defoliated 1987 and 1988	284,853	18,704	49,924	4,876	462,428
Defoliated 1987 only	13,348	34,950	620	3,529	52,329
Defoliated 1988 only	104,120	3,771	132,809	4,254	141,001
Defoliated 1987 and 1988	0	0	0	0	0
Totals	402,321	57,425	183,352	12,659	655,758

Spectral-Temporal Error Matrix, Reference Data

Classified Data	Non-Def. 1987/88	Defol. 1987	Defol. 1988	Defol. 87/88	Totals
Non-Defoliated 1987 and 1988	327,562	34,891	125,989	4,605	493,047
Defoliated 1987 only	15,609	16,127	603	3,215	35,554
Defoliated 1988 only	49,667	5,445	55,414	3,359	113,885
Defoliated 1987 and 1988	9,483	962	1,347	1,480	13,272
Totals	402,321	57,425	183,352	12,659	655,758

PCCDD Error Matrix, Reference Data

Classified Data	Non-Def. 1987/88	Defol. 1987	Defol. 1988	Defol. 87/88	Totals
Non-Defoliated 1987 and 1988	294,168	20,722	90,488	5,120	410,
Defoliated 1987 only	10,496	18,459	717	1,503	31,175
Defoliated 1988 only	86,371	6,978	91,289	4,360	188,998
Defoliated 1987 and 1988	11,286	11,266	859	1,676	25,087
Totals	402,321	57,425	183,352	12,659	655,758

Where: values are pixels classified.

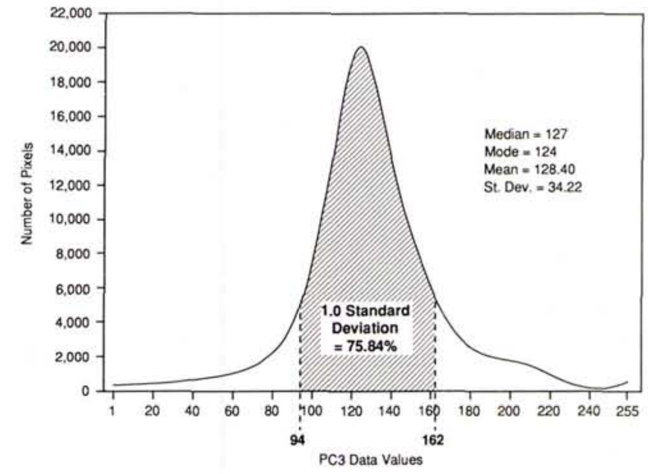

Figure 4. PC3 smoothed frequency polygon with 1.0 standard deviation values.

and data reduction, with results comparable to PCA. ID is computationally very simple and easy to interpret. Band-by-band subtraction permits the analysis of the nature of inter-image change on a per-band basis.

Spectral-Temporal Change Classification

STCC proved to be the most analytically intensive of the techniques studied. Because the data sets are merged and no preprocessing is prescribed for data reduction, it is necessary to analyze all bands to subset the data. Signature development

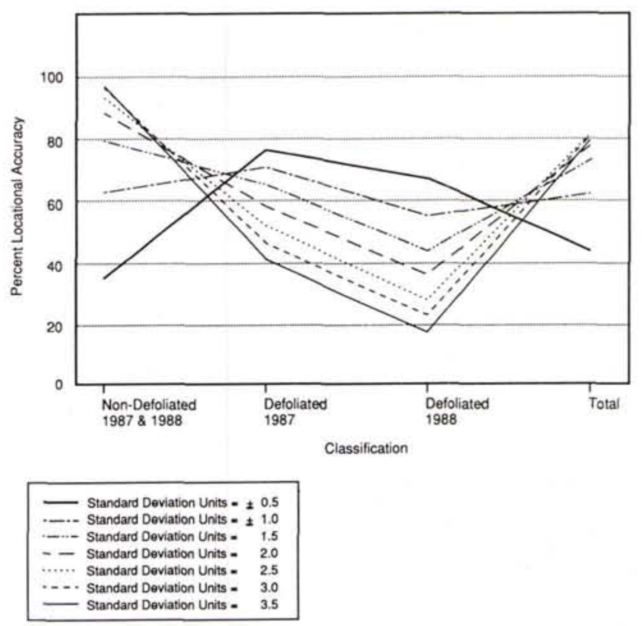

Figure 5. PC3 level slice accuracies.

TABLE 3. TEST OF AGREEMENT

Error Matrix	Accuracy	Normalized Accuracy	Khat	Variance
Merged PCA	0.6332	0.6074	0.2494	0.00001272
PCA Eigenimage 3	0.6561	0.6849	0.3629	0.00001234
Image Differencing	0.6902	0.7418	0.4542	0.00001101
Spectral-Temporal	0.6109	0.6159	0.2064	0.00001305
Post-Classification	0.6185	0.6664	0.3052	0.00001399

TABLE 4. PAIR-WISE SIGNIFICANCE TEST FOR ERROR MATRICES BY TECHNIQUE AT 95 PERCENT-CONFIDENCE INTERVAL (± 1.96)

Techniques by Pair	Test Statistic	Result
MPCA — PC3	−22.6678	Significant
MPCA — ID	−42.0261	Significant
MPCA — STCC	8.4676	Significant
MPCA — PCCDD	−9.3698	Significant
PC3 — ID	−18.8887	Significant
PC3 — STCC	31.0517	Significant
PC3 — PCCDD	12.6759	Significant
ID — STCC	50.5003	Significant
ID — PCCDD	31.2595	Significant
STCC — PCCDD	−17.5787	Significant

for change detection using STCC is complex because multidate change signatures, and not just defoliation signatures, must be developed.

Post-Classification Change Detection Differencing

PCCDD is the most straightforward technique because the data remain in image format. It does not, however, allow for normalizing differences between multitemporal data caused by sensor and atmospheric influences, and care must be taken so that non-feature changes are not classified as change. The primary disadvantage of PCCDD is that, although it is possible to standardize classification procedures from one data set to another, the technique does not allow for normalizing differences between multitemporal data attributable to sensor and atmospheric influences.

Conclusions

Principal components analysis and image differencing offer the greatest potential for achieving reliable mapping of defoliation. That a density level slice of a single principal component could be used to characterize changes due to defoliation is an outcome of special interest. When used in conjunction with ground and aerial photography-based assessment methods, change detection using satellite-borne remote sensing data may aid in the systematic and quantitative monitoring of defoliation conditions.

A limitation to using a change detection approach to identify and monitor defoliation is that, if defoliation occurs in the same area during consecutive years, there will be no net change during that period. However, once baseline conditions are established, monitoring can proceed normally.

Digital change detection offers potential benefits for monitoring defoliation over large areas. Image differencing and principal components analysis are rather straightforward and could be automated easily. Even if defoliation could not be readily classified, the detection of change could be referenced in a spatial database to isolate change occurring in hardwood forests, thus effectively reducing sampling costs required for other monitoring techniques.

Acknowledgments

The authors wish to thank Dr. Mark Lindberg of the University of South Florida and Dr. Robert Rundstrom of the University of Oklahoma, Mr. William Clerk and Mr. Robert Acciavatti of the U.S. Forest Service Forest Pest Management Section, and Mr. John Coleman, District Ranger of the Lee Ranger District of the George Washington National Forest, for their support of this research.

References

Aldrich, R.C., 1975. Detecting Disturbances in a Forest Environment, *Photogrammetric Engineering & Remote Sensing*, 41:39–48.

Aldrich, R.C, R.C. Heller, and W.F. Bailey, 1958. Observation Limits for Aerial Sketch-Mapping Southern Pine Beetle Damage in the Southern Appalachians, *Journal of Forestry*, 56(3):200–202.

Bryant, E., A.G Dodge, Jr., and S.D. Warren, 1980. Landsat for Practical Forest Type Mapping: A Test Case, *Photogrammetric Engineering & Remote Sensing*, 46:1575–1584.

Buchheim, M.P., A.L. Maclean, and T.M. Lillesand, 1984. Forest Cover Type Mapping and Spruce Budworm Defoliation Using Simulated SPOT Imagery, *SPOT Simulation Applications Handbook*, Proceedings of the 1984 SPOT Symposium, American Society of Photogrammetry and Remote Sensing, Falls Church, Virginia, pp. 259–266.

Byrne, G.F., P.F. Crapper, and K.K. Mayo, 1980. Monitoring of Land-Cover Change by Principal Components Analysis of Multitemporal Landsat Data, *Remote Sensing of Environment*, 10:175–184.

Christenson, J.W., and H. Lachowski, 1976. Urban-Area Delineation and Detection of Change Along the Urban-Rural Boundary as Derived from Landsat Digital Data, *Proceedings of the Fall Meeting of the American Society of Photogrammetry, American Society of Photogrammetry*, Falls Church, Virginia, pp. 28–33.

Ciesla, W.M., 1981. Development and Application of Panoramic Aerial Photography in Forest Pest Management, *Eighth Biennial Workshop on Color Aerial Photography in the Plant Sciences and Related Fields*, SAF, ASP, and VPI, Luray, Virginia, 21–23 April, pp. 19–29.

Ciesla, W.M., C.W. Dull, and R.E. Acciavatti, 1989. Interpretation of SPOT-1 Color Composites for Mapping Defoliation of Hardwood Forests by Gypsy Moth, *Photogrammetric Engineering & Remote Sensing*, 55:1465–1470.

Coiner, J.C., 1980. Using Landsat to Monitor Changes in Vegetation Cover Induced by Desertification Processes, *Symposium on Remote Sensing of Environment*, Environmental Research Institute of Michigan, Ann Arbor, Michigan, 3(14):1341–1347.

Congalton, R.G., 1991. A Review of Assessing the Accuracy of Classifications of Remotely Sensed Data, *Remote Sensing of Environment*, 37:33–46.

Congalton, R.G., R.G. Oderwald, and R.A. Mead, 1983. Assessing Landsat Classification Accuracy Using Discrete Multivariate Analysis Statistical Techniques, *Photogrammetric Engineering & Remote Sensing*, 49(12):1671–1678.

Duggin, M.J., R. Rowntree, M. Emmons, N. Hubbard, A.W. Odell, H. Sakhavat, and J. Lindsey, 1986. The Use of Multidate Multichannel Radiance Data in Urban Feature Analysis, *Remote Sensing of Environment*, 20:95–105.

Duvernoy, J., and J. Leger, 1980. Karhunen-Loeve Analysis of Multispectral Data From Landscapes, *Optics Communications*, 32(1): 39–44.

Estes, J.E., D. Stow, and J.R. Jensen, 1982. Monitoring Land Use and Land Cover Changes, *Remote Sensing for Resource Management* (C. Johannsen and J. Sanders, editors), Soil Conservation Society of America, Ankeny, Iowa, pp. 100–110.

Franklin, S.E., 1989. Classification of Hemlock Looper Defoliation

Using SPOT HRV Imagery, *Canadian Journal of Remote Sensing*, 15(3):178–182.

Fung, T., and E. LeDrew, 1987. Application of Principal Components Analysis to Change Detection, *Photogrammetric Engineering & Remote Sensing*, 53(12):1649–1658.

Holmes, R., D. Wagner, and D. Racey, 1984. *Soil Survey of Warren County, Virginia*, U.S. Department of Agriculture Soil Conservation Service in cooperation with Virginia Polytechnic Institute and State University, Washington, D.C.

Hong, J-K, and J. Iisaka, 1982. Coastal Environment Change by Landsat MSS Data, *Remote Sensing of Environment*, 12:107–116.

Jensen, J.R, 1986. *Introductory Digital Image Processing*, Prentice Hall, Englewood Cliffs, New Jersey.

Jensen, S.K., and F.A. Waltz, 1979. Principal Components Analysis and Canonical Analysis in Remote Sensing, *Proceedings of the 45th Annual Meeting of the ASP*, 18–24 March, Washington, D.C., 1:337–348.

Johnson, G.R., 1980. Mapping Hardwood Forest Defoliation by Digital Analysis of Satellite Data, *Remote Sensing of Earth Resources, Vol. VII* (F. Shahrokhi, editor), University of Tennessee, Tullahoma, Tennessee, pp. 139–157.

Knight, F.B., and H. J. Heikkenen, 1980. *Principals of Forest Entomology*, McGraw-Hill, New York, pp. 240–242.

Nash, A.J., J.R Seifert, and G.M. Schoen, 1980. Forest Cover Mapping from Landsat Imagery, *Remote Sensing of Earth Resources Vol. VII* (F. Shahrokhi, editor), University of Tennessee Space Institute, Tullahoma, Tennessee, pp. 129–137.

Nelson, R.F., 1983. Detecting Forest Canopy Change Due to Insect Activity Using Landsat MSS, *Photogrammetric Engineering & Remote Sensing*, 49:1303–1314.

Robinove, C.J., Jr., P.S. Chavez, Jr., D. Gehring, and R. Holmgren, 1981. Arid Land Monitoring Using Landsat Albedo Images, *Remote Sensing of Environment*, 11:133–156.

Rohde, W.G., and H.J. Moore, 1974. Forest Defoliation Assessment with Satellite Imagery, *Proceedings of the Symposium on Remote Sensing of Environment*, Environmental Research Institute of Michigan, Ann Arbor, Michigan, 2(9):1089–1104.

Sader, S.A, 1987. Digital Image Classification Approach for Estimating Forest Clearing and Regrowth Rates and Trends, *Proceedings of IGARSS '87 Symposium*, Ann Arbor, Michigan, 18–21 May, pp. 209–213.

Sirois, J., and F.J. Ahern, 1989. An Investigation of SPOT HRV for Detecting Recent Mountain Pine Beetle Mortality, *Canadian Journal of Remote Sensing*, 14(2):104–110.

Smith, D.W., and N.E. Linnartz, 1980. The Southern Hardwood Region, *Regional Silviculture of the United States* (John W. Barrett, editor), John Wiley & Sons, New York, N.Y., pp. 145–238.

Talerico, R.L., J.E. Walker, and T.A. Skratt, 1978. Quantifying Gypsy Moth Defoliation, *Photogrammetric Engineering & Remote Sensing*, 44:1385–1392.

Tom, C.H., and L.D. Miller, 1980. Forest Site Index Mapping and Modeling, *Photogrammetric Engineering & Remote Sensing*, 46: 1585–1596.

Vogelmann, J.E., 1989. Use of Thematic Mapper Data for the Detection of Forest Damage Caused by the Pear Thrips, *Remote Sensing of Environment*, 30:217–225.

Vogelmann, J.E., and B.N. Rock, 1988. Assessing Forest Damage in High-Elevation Coniferous Forests in Vermont and New Hampshire Using Thematic Mapper Data, *Remote Sensing of Environment*, 24:227–246.

Weismiller, R.A., S.J. Kristof, D.K. Scholz, P.E. Anuta, and S.M. Momin, 1977. Evaluation of Change Detection Techniques for Monitoring Coastal Zone Environments, *Symposium on Remote Sensing of Environment*, Environmental Research Institute of Michigan, Ann Arbor, Michigan, 2(11):1229–1235.

Wickware, G.M., and P.J. Howarth, 1981. Change Detection in the Peace-Athabasca Delta Using Digital Landsat Data, *Remote Sensing of Environment*, 11:9–25.

Williams, D.L., and R.F. Nelson, 1986. Use of Remotely Sensed Data for Assessing Forest Stand Conditions in the Eastern United States, *IEEE Transactions on Geoscience and Remote Sensing* GE-24(1):130–138.

Williams, D.L., R.F. Nelson, and C.L. Dottavio, 1985. A Georeferenced LANDSAT Digital Database for Forest Insect-damage Assessment, *International Journal of Remote Sensing*, 6(5):643–656.

(Received 8 February 1991; revised and accepted 1 April 1993)

Douglas Muchoney

Douglas Muchoney is an Ecologist/Remote Sensing Specialist at the International Headquarters of The Nature Conservancy. His degrees are in Forestry (B.S., Virginia Polytechnic Institute, 1982) and Geography/Cartography (M.S., George Mason University, 1991). He specializes in integrated remote sensing and GIS for the characterization and monitoring of biodiversity and the terrestrial environment.

Barry Haack

Barry Haack is an Associate Professor of Geographical and Cartographical Sciences at George Mason University in Fairfax, Virginia. His graduate work was in geography at San Diego State University and the University of Michigan. His primary research interest is the application and technology transfer of remote sensing and associated techniques for resource assessment and monitoring.